ISSN 1726-5479

SENSORS & TRANSDUCERS

vol. 95
8/08

Sensors and Transducers Applications

International Frequency Sensor Association Publishing

IFSA

Sensors & Transducers

Volume 95
Issue 8
August 2008

www.sensorsportal.com

ISSN 1726-5479

Sensors & Transducers Journal

Contents

Volume 95
Issue 8
August 2008

www.sensorsportal.com

ISSN 1726-5479

Research Articles

Authors are encouraged to submit article in MS Word (doc) and Acrobat (pdf) formats by e-mail: editor@sensorsportal.com
Please visit journal's webpage with preparation instructions: http://www.sensorsportal.com/HTML/DIGEST/Submition.htm

International Frequency Sensor Association (IFSA).

Sensors & Transducers Journal, Vol. 95, Issue 8, August 2008, pp. 108-127

Sensors & Transducers

ISSN 1726-5479

http://www.sensorsportal.com

Development of Portable Phonocardiographic Fetal Heart Rate Monitor

Jianfeng CHEN, Koksoon PHUA, Ying SONG
Institute for Infocomm Research
21 Heng Mui Keng Terrace, Singapore 119613
Tel.: +65-68748401
E-mail: ksphua@i2r.a-star.edu.sg

Received: 31 March 2008 /Accepted: 15 August 2008 /Published: 25 August 2008

Abstract: In this paper we present a portable PDA-based fetal heart monitor that is able to provide instantaneous fetal heart rate (FHR) for pregnant women. Several signal processing techniques are implemented in the device to make it clear, reliable and ease-to-use. A modified spectral subtraction algorithm is first used to remove the unwanted stationary background noise from the noisy fetal heart sound. The AM/FM modulation technique is then employed to make the fetal heart sound more audible so that both pregnant women and gynecologists can identify the rhythmic fetal heart beat sounds easily. A real-time algorithm is proposed to extract the fetal heart rate information from the weak and noisy signals. Furthermore, based on the signal spectrum distribution, a confidence factor (CF) is designed to indicate the reliability of the estimated fetal heart rate in real time. In turn, CF can also be used to guide the user to locate the optimum auscultation position during the initial search stage. The device has been tested in a local hospital on a sample group of 41 pregnant women. Our finding shows that an approximate 75 % of the pregnant mothers are able to hear their baby's heart sound clearly using our device. Tests are also carried out to compare the fetal heart rate calculated using our device and the existing ultrasound cardiotocography (CTG) machine. In most time our device functions properly and provides results close to the CTG records. *Copyright © 2008 IFSA.*

Keywords: Fetal heart monitoring, Phonocardiographic, Fetal heart rate, Biomedical signal processing

---

1. Introduction

Monitoring the variations in the fetal heart rate (FHR) provides up-to-date information about the general well-being of the fetus inside mother's womb. Hence, long term FHR recording and evaluation is essential, particularly during the last week of pregnancy and labour, to identify fetal distress and decide if intervention such as caesarean section is necessary [1]. In obstetrics clinic and hospital, the traditional fetal surveillance relies heavily on ultrasonic techniques such as the cardiotocography (CTG) system. The ultrasonic system involves the transmission of ultrasound signals which, when reflected from the fetus, provides an indication of the fetal situation awareness. However, frequent and long time exposure to the ultrasound radiation is not recommended for both mother and fetus and thus not suitable for long term fetal monitoring. In addition, CTG systems require a high level of expertise and experience to acquire the necessary information [2]. Even for hand-held ultrasound Doppler-based devices accurate sensor alignment is required for an expert to obtain the correct FHR.

Many efforts have been made to find alternatives to the ultrasonic diagnostic means. Among these are the fetal electrocardiography (fECG), the fetal magnetic cardiography (fMCG) and the fetal phonocardiogram (fPCG), which are all passive in nature. The fECG uses electrodes placed on the maternal abdominal surface for FHR monitoring and its performance depends on the proper placement of the multiple electrodes by professionals. As the electrodes need to be adjusted from time to time, this method is not convenient for long-term recording [3]. It was also reported that during certain period of pregnancy (24-36 weeks), the false alarm rate of fECG is quite high for FHR measurement. The fMCG, on the other hand, utilizes big and expensive magnetic equipment to sense the fetal heart induced magnetic signature and thus is not suitable for long term monitoring as well, especially in the environments like home or office.

The fPCG signals are produced by the opening and the closing of the fetal heart valves and are captured by simply placing an acoustic sensor on the mother’s abdomen. Compared with above mentioned techniques, the fPCG has two distinct advantages. Firstly, the fPCG offers a complete non-invasive means of fetal assessment. Being a passive system, no energy is emitted at all and it eliminates the risk of harmful exposure to both mothers and babies. Secondly, the fPCG signals can be conveniently captured by placing a small acoustic sensor on mother’s abdomen without the use of gel as in the CTG monitor. The energy requirement and the size are also trivial, which in turn offers greater portability. This promises the potential of home use and facilitates portable implementation.

On the other hand, there are two technical issues hindering the use of fPCG in practice. Due to the nature of the fetal heart sound, the acoustic sensor must be sensitive enough to pick up the weak and low frequency (35-110 Hz) vibrations from the maternal abdominal surface. Secondly, the signal processing methods must be robust enough to calculate the FHR from the fetal heart sound which are contaminated by various maternal organ sounds, the fetal movements and breathing sound, the shear noise caused by the measurement head movement during recording, and the environmental noises, etc.

The majority of the early works in this area are focused on sensor development [5-11]. In order to pick up the fetal heart sound efficiently, various types of sensors and structures have been proposed, including the cantilever accelerometer [5], the inductive sensor [7] and the piezoelectric microphone [8], etc. Recently, the miniature electret microphones have also been attempted with reasonably good performance [3-4]. More recent studies, on the other hand, concentrated on FHR estimation. Some examples are the band pass filtering [12], the linear cross correlation [2] or the variable comb filtering [13], etc. However, most of these methods could not deal with the noisy fetal heart signal in the presence of various nonstationary interferences. Thus, a series of carefully designed rules such as those presented in [3-4] were proposed to overcome the problem. Despite these efforts, only a handful of these techniques progressed beyond the stage of research to become a practical application instrument that is suitable for clinical or home use. Among these techniques is the prototype from NASA Langley research centre and the works conducted by Technical university of Budapest. In [24], it was reported that QXCI has developed an fPCG type fetal status monitoring system called FETAPHONE QX, which costs thousands of dollars and yet requires the supervision of a professional operator.

There is, no doubt, a gap between the existing technologies and the user requirements for a cheap, safe, convenient and reliable fetal heart monitoring device. Motivated by these needs, we conducted our study specifically on the fetal heart sound *audibility enhancement*, the FHR *calculation under real situation* and the *instantaneous FHR result evaluation*. The work was finally implemented on a HP iPaq hx4700 and had been tested on a group of 41 pregnant women in a local hospital.

The paper is organized as follows. In Section 2, we introduce the structure of the proposed system and the detailed function of each module, namely the modified spectral subtraction, the AM/FM modulation, the FHR calculation method and a confidence factor for FHR evaluation. A PDA based implementation is described and the detailed clinical trail results are reported in Section 3. Finally in Section 4, we will make our conclusions.

2. Proposed System

The block diagram of the proposed system is depicted in Fig. 1. An electret microphone is used to capture the fetal heart sound and attached to an inverse-horn-shaped [1] cone to match the acoustic impedance between the microphone and the mother abdominal surface. The weak fetal heart signal from the microphone is then amplified by a low noise pre-amplifier, filtered by an 8-order low-pass filter and then digitized for the subsequent processing.

To enable the user to hear the heart beat rhythm clearly and easily, we employ a noise reduction process followed by an AM/FM modulation. A computational efficient spectral subtraction algorithm [31-32] for nonstationary signal enhancement is customized to make the desired fetal heart sound more distinct. The AM/FM modulation produces more audible fetal heart sound that makes it easier for the user to locate the strongest fetus heart auscultation location on the mother abdomen. The processed digital signal is then converted back into the analog signal and amplified further to drive an earphone or a loudspeaker.

Meanwhile, a FHR calculation method is proposed which is highly computational efficient so that the algorithm can be implemented using a simple microcontroller or in a PDA. It was found that the non-linear processing on the fetal heart sound imposed by the abovementioned noise reduction method will affect the accuracy of the FHR calculation. For this reason, the original signal $z[k]$ is directly used for the FHR calculation, as shown in the right side of Fig. 1. In addition, a confidence factor is proposed with score ranging from 0 (least reliable) to 1 (most reliable) to indicate the reliability of the FHR result. A detailed description of each module will be explained in the following sub-sections respectively.

2.1. Analog and Digital Preprocessing

As reported in [4], the main components of the fetal heart sound fall into 35-110 Hz. Hence, 8-order low pass analog filters chip (MAX7400) working at 110 cut-off frequency was further used in our analog support circuit. After sampling at Fs, the captured discrete fetal heart sound signal $x[k]$ is then filtered using an 8-order Butterworth-type high pass IIR digital filter to attenuate components below 35 Hz. The resulting filtered signal $y[k]$ is given by

$$z[k] = \sum_{i=0}^{n_b+1} b[i]x[k-i] - \sum_{i=2}^{n_a+1} a[i]z[k-i], \qquad (1)$$

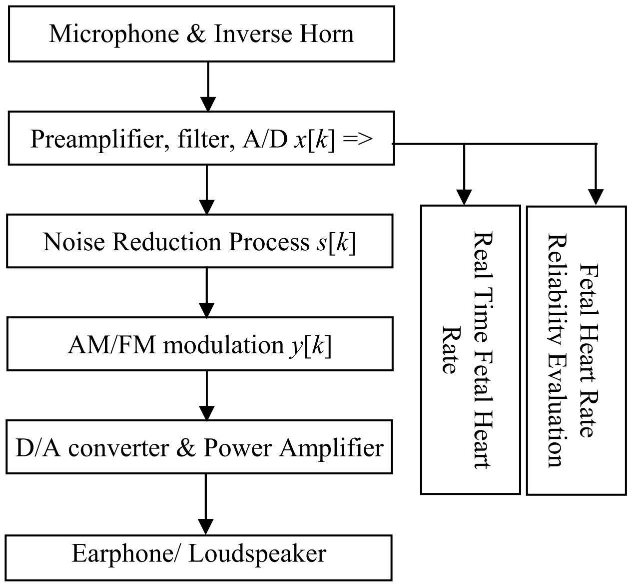

Fig. 1. Block diagram of the proposed system.

where n_a and n_b are the filter length and set to be 8 in our prototype, ***a*** and ***b*** are the filter coefficient vectors, given by

a = [1.000 -7.7182 26.0669 -50.3159 60.7125 -46.8930 22.6409 -6.2477 0.7544]

b = [0.8686 -6.9484 24.3195 -48.6390 -60.7987 -48.6390 24.3195 -6.9484 0.8686].

It should be noted that both the analog and digital filters can only remove those noises outside the filtering passband. In the next section a frequency domain operation will be conducted to remove those stationary noises whose spectrum overlap with the desired signals.

2.2. Simplified Spectral Subtraction

Researchers have proposed a number of noise reduction methods for *adult* heart sound signals, for example, averaging [25], adaptive filtering [26-28], wavelet-based method [29] and their integration [30]. However, most of them may not be suitable for the fetal heart sound signal. For example, the averaging method may fail because it is very difficult to identify the individual heart beat cycles and their respective margins. The adaptive filtering may not perform well as the complexity of the interference signal sources and the unknown noise and signal propagation path make it impossible to get a good reference signal. The wavelet-based method relies on the selection of the proper wavelet package. Due to the large variation and highly non-stationary of the fetal heart sound signals, any single wavelet could be incompetent in performing this task and the procedure of wavelet selection is also problematic [29-30].

To further reduce the noises whose spectrum overlap with that of the fetal heart sound, we propose to use a modified spectral subtraction method [31-32] originated from the speech enhancement techniques, which is suitable for attenuating the stationary noise from the non-stationary signal, e.g., speech, fetal heart signal, etc. Furthermore, we will explore some priori knowledge of the fetal heart sound signals to facilitate the original method implementation. A diagram for the algorithm is shown in Fig. 2.

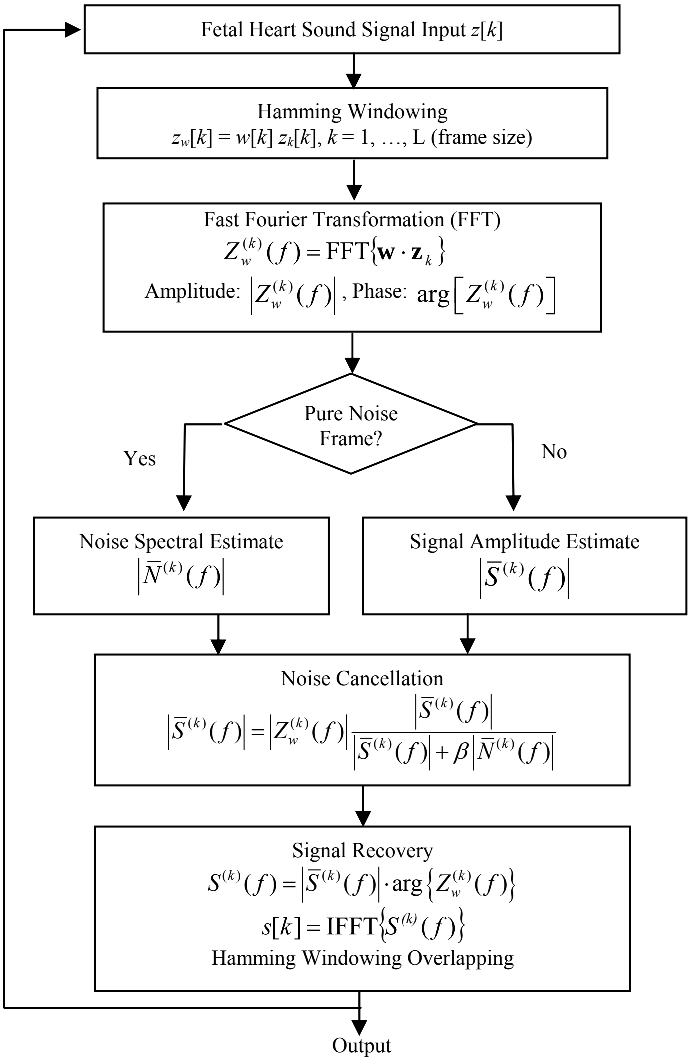

Fig. 2. Flowchart of the modified spectral subtraction method.

The noisy signal is modeled as

$$z[k] = s[k] + n[k], \tag{2}$$

where $z[k]$, $s[k]$ and $n[k]$ denote the original noisy fetal heart signal, the expected clean signal and the additive background noise, respectively. The procedure of the algorithm is summarized as follows.

Step 1: The data is processed in batch mode. The sampled data is first divided into short frames. To prevent spectral leakage and to ensure signal continuity, each frame is Hamming windowed with 50% overlapping. Then the frequency response of the windowed k^{th} frame signal is obtained by using the Fast Fourier Transform (FFT) as

$$Z_w^{(k)}(f) = FFT\{w \bullet z_k\}, \tag{3}$$

where (·) represents the vector dot multiply operator, z_k denotes the original signal vector of kth frame, w denotes the Hamming window vector. Unlike speech signal, the fetal heart sound signal is periodical and composed of two short pulses (S_1 and S_2) and a large portion of noise. To explore this *a priori* feature, we set the frame size to be 30 ms, which is less than one tenth of a normal fetal heart period (300-600 ms). Hence, there must be some frames containing no fetal heart sound, which can be readily used for noise estimation. This significantly reduces the complexity of the original method [31-32].

Step 2: Based on the spectral energy statistics [31-32], we can determine whether the current frame contains 'pure noise'. If yes, the amplitude of the noise spectrum $\left|\overline{N}^{(k)}(f)\right|$ is updated by

$$\left|\overline{N}^{(k)}(f)\right| = \alpha\left|\overline{N}^{(k-1)}(f)\right| + (1-\alpha)\left|Z_w^{(k)}(f)\right|, \tag{4}$$

while the amplitude of the signal spectral $\left|\overline{S}^{(k)}(f)\right|$ remains the same,

$$\left|\overline{S}^{(k)}(f)\right| = \left|\overline{S}^{(k-1)}(f)\right|, \tag{5}$$

Otherwise, $\left|\overline{S}^{(k)}(f)\right|$ is updated

$$\left|\overline{S}^{(k)}(f)\right| = \alpha\left|\overline{S}^{(k-1)}(f)\right| + (1-\alpha)\max\left\{\left[\left|Z_w^{(k)}(f)\right| - \beta\left|\overline{N}^{(k-1)}(f)\right|\right], 0\right\}, \tag{6}$$

while $\left|\overline{N}^{(k)}(f)\right|$ remains the same,

$$\left|\overline{N}^{(k)}(f)\right| = \left|\overline{N}^{(k-1)}(f)\right|, \tag{7}$$

In Eq. (4) and (6), the parameter α denotes the forgetting factor used to control the updating speed of the signal and noise spectral amplitude. α normally is selected as a positive number less than but close to 1, such as 0.95. On the other hand, the parameter β controls the amount of noise subtracted from the windowed noisy signal $|Z_w(f)|$. For full noise subtraction β is set to be 1 and for under-subtraction β can be less than 1.

Step 3: The amplitude of $Z_w^{(k)}(f)$ is attenuated according to the estimated signal-to-signal-plus-noise ratio. The resulted *clean* signal is given by

$$\left|\overline{S}^{(k)}(f)\right| = \left|Z_w^{(k)}(f)\right| \frac{\left|\overline{S}^{(k)}(f)\right|}{\left|\overline{S}^{(k)}(f)\right| + \beta\left|\overline{N}^{(k)}(f)\right|}, \tag{8}$$

$$\arg[\overline{S}^{(k)}(f)] = \arg\left\{Z_w^{(k)}(f)\right\}, \tag{9}$$

where $\left|S^{(k)}(f)\right|$ is an estimate of the clean signal spectrum magnitude and arg{} denotes the phase operator.

Step 4: Recover the signal by applying the Inverse Fast Fourier Transformation (IFFT).

$$S^{(k)}(f) = \left|\overline{S}^{(k)}(f)\right| \cdot \arg\left\{Z_w^{(k)}(f)\right\}, \tag{10}$$

$$s[k] = \text{IFFT}\left\{S^{(k)}(f)\right\}, \tag{11}$$

As mentioned earlier, the noises in the fetal heart sound include both stationary and nonstationary sources. For stationary noise, such as the slow variant organ movement noise and the electric self-noise, this modified spectral substraction method performs well. The processed signal looks much cleaner and sounds clearer as well. However, this method is not effective in removing nonstationary noises, such as some occasional burst or impulse-like noises, and the maternal heart beat. Nevertheless, it has been found that since the rhythm of the fetal heart beat is periodical and much faster than the maternal heart rate, the negative effect of these nonstationary noises on the identification of the fetal heart beat is insignificant. Experiments to illustrate the effectiveness of the modified spectral subtraction will be given in section 3.

2.3. AM/FM Modulation

The sensitivity of the human hearing varies significantly across the whole audible frequency band 20-20000 Hz. The human ears are most sensitive to the frequency in about 4 kHz and are insensitive to the low frequency from 100 Hz downward and high frequency from 16 kHz upward [34]. This is one of the reasons why people cannot easily hear and identify the fetal heart sound, which mainly falls below 100 Hz.

2.3.1. Amplitude Modulation

One way to make the low frequency fetal heart sound more audible is to shift the low frequency components to a higher band while keeping the rhythm unchanged. This can be realized through an amplitude-modulation (AM) process. This approach can also be found in the earlier works that use the modulation technique to monitor the low frequency whale or dolphin sound for their vocalization identification. Based on the human ear sensitivity chart as in [34], when we shift a base band signal (35-150 Hz) 250 Hz higher, the audibility of the signal can be regarded as being amplified by 20-40 dB or 100-10000 times in energy. Such effect cannot be achieved directly by amplifying the original signals due to the dynamic range limitation of the circuitry and the normal earphone and loudspeaker.

The AM can be carried out by using the Single Side Band Modulation (SSB) [36]. Following the previous module, in this sub-section we manipulate on the $s[k]$ resulted from Eq. (11). Assuming one of its frequency components is f_0, the spectrum of $s[k]$ can be shifted higher by f_C and resulting in a final frequency of $f_1 = f_0 + f_C$. The process can be described as follows.

The multiplication between $s[k]$ and the carrier signal is obtained first by

$$y'[k] = s[k]\cos\left(\frac{2\pi f_c k}{F_s}\right), \tag{12}$$

where F_s is the sampling rate. The spectrum of this transform is

$$Y'(f) = \frac{S(f+f_c)+S(f-f_c)}{2}, \tag{13}$$

where S(f) denotes the spectrum of $s[k]$. If we design a high pass filter as

$$H(f) = \begin{cases} 1 & \text{for} \left| f \right| > f_c \\ 0 & \text{elsewhere} \end{cases}, \quad (14)$$

As a result, we will have

$$Y(f) = Y'(f)H(f) = 0.5S(f + f_c), \quad (15)$$

The output $y(t)$ is the Inverse Fast Fourier Transform of $Y(f)$, i.e.,

$$y[k] = \text{IFFT}\{Y(f)\}, \quad (16)$$

To determine the modulation frequency, three issues are taken into consideration, which are the sampling rate, the audibility and the experience of the users. Based on our experiments and the feedbacks from many testers, an appropriate modulation frequency f_C was found to be within the range of 150 - 250 Hz.

2.3.2. Frequency Modulation

The Doppler devices obtain the fetal heart information by using the detected contraction speed of the fetal heart surface [35], from which the FHR can be calculated and the audio output represented as in Eq. (17) can be played out.

$$x(t) = \cos\left[2\pi f_0 (2/c)\cos\theta \cdot \left| v \right| \cdot \mathrm{t}\right], \quad (17)$$

where f_u is the frequency of the radiated ultrasound wave and c the propagation speed of the ultrasound in the medium. The detected organ is moving at the velocity v at the angle θ with the ultrasound source. Eq. (17) is essentially a frequency modulation (FM) process by which the high velocity instants are presented as high frequency signals and vice versa. On the other hand, although the heart contraction cycle exactly synchronize with the heart sound cycle, it should be emphasized that the Doppler audio sound is purely constructed from the fetal heart movement and does not contain any heart sound related information which may have potentials in heart problem diagnosis as in adult heart sound auscultation.

Gynecologists are more accustomed to the sound produced by their familiar ultrasound devices. Therefore we can make use of the FM technique to construct the fetal heart sound similar to that of the Doppler device. If the modulation frequency and the working frequency band are selected properly, in terms of the audibility the strong signals will become much audible as opposed to the weak signals. The envelop of the modulated waveform is completely different from that of the original signal and only the instantaneous frequency of the modulated signal reflects the original signal. The transformed signal is of the form

$$y(k) = A\cos\left(2\pi f_c t + k\int_0^t S(t)dt\right)\Big|_{t=k/F_s}, \quad (18)$$

where f_C is the carrier frequency and κ the frequency deviation of the modulation. One can refer to [36] for more detailed information on implementation of the FM.

2.4. Fetal Heart Rate Calculation

For high quality fetal heart sound, in each cycle a distinct first heart sound S_1 and a second heart sound S_2 can be located in the waveform. When this is not the case, a set of rules were designed [3-4] to ensure that each S_1 and S_2 are well matched and therefore a reliable heart beat cycle can be identified. However, when the fetal heart sound is even worse and the S_1 and S_2 are completely un-recognizable (see Fig. 3b), the methods in [3-4] will produce many unreliable results. In light of this, we propose not to match S_1 and S_2 peaks but to search the most likely S_1 peaks only. The method can thus work on much wider range of signals with different level of quality. Here we should be reminded that although the previous modules in 2.2-2.3 enhance the listening experience of the fetal heart beat, they are non-linear processing in nature and may introduce negative effect in the fetal heart rate calculation, especially in low signal-to-noise-ratio cases. Hence, we will directly use the $z[k]$ obtained in Eq. (1) to calculate the FHR.

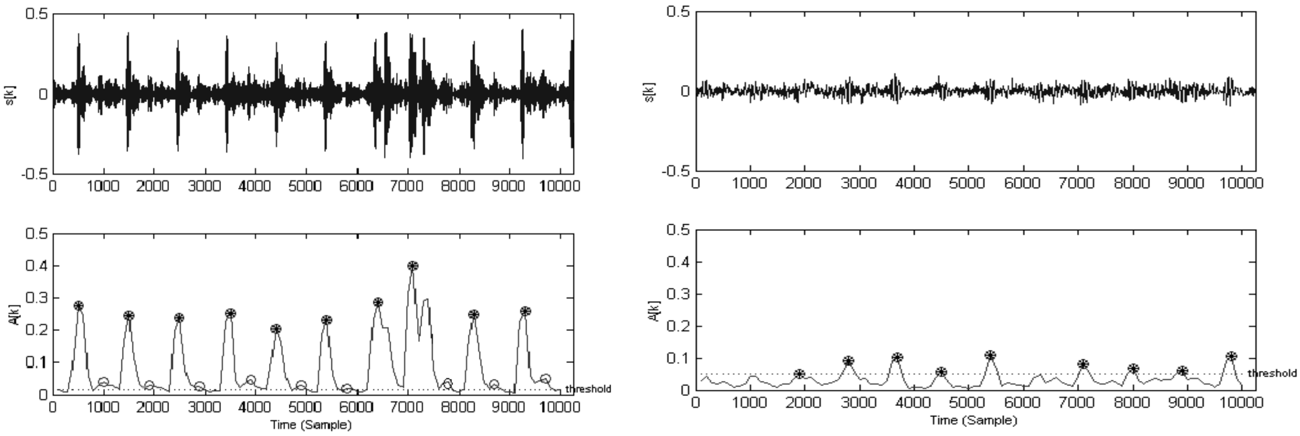

(a) (b)

Fig 3. Two 5-seconds fetal heart sound signals (top) and their envelop $A[k]$ (below). The sampling rate is Fs = 2000 Hz. The circles 'o' stand for all the qualified peaks and the stars '*' stand for the selected S1 peaks.
(a) a segment of strong signal with distinct peaks and little interference;
(b) a segment of weak signal and low SNR.

2.4.1. Amplitude Envelop

For diagnosis purpose, instantaneous beat-to-beat FHR is more valuable than long term averaging FHR. In practice, each FHR result is obtained as an average value over a short period, e.g., 3 seconds, assuming that there would be little changes during this period [3-4].

To obtain the beat-to-beat FHR, we first calculate the amplitude envelop, $A[k]$, of the signal $z[k]$ by

$$A[k] = \sqrt{\frac{1}{L}\sum_{j=k}^{k+L-1} z^2[j]}, \quad (19)$$

where L is the frame size for envelop calculation. Given sampling rate Fs = 2000 Hz, we choose $L = 200$ which is equivalent to 100ms in time. In the following, every FHR result, FHR[k], will be obtained based on a 3-second segment of the $A[k]$ envelop. The segments window can be shifted with overlapping such that the FHR results can be updated more frequently and smoothly.

2.4.2. Peak Localization

From Fig. 3 we can see that the distinct peaks in the envelop can clearly depict the fetal heart beat cycles. To locate these peaks, we set a threshold first to exclude those trivial peaks with much lower amplitude. For strong and high quality fetal heart sound, like the one shown in Fig. 3(a), the distinct peaks are easy to locate and the threshold is normally set to a small constant value. But for those with lower SNR and poor quality, an adjustable threshold is designed to reject those trivial peaks. The threshold A_{Thrd} is defined as

$$A_{Thrd} = \begin{cases} \overline{A} + 0.80\delta_A & \text{if } \overline{A} < 0.75A_0 \\ A_0 & \text{otherwise} \end{cases}, \tag{20}$$

where $\overline{A}$ and δ_A is the mean and the standard deviation of $A[k]$. A_o represents a fixed small value such as 0.001. The value 0.80, 0.75 and 0.001 are all empirically obtained through our experiments.

Next, the peaks at instant p_i are determined by using the rules as follows

$$A[p_i] \geq A_{Thrd} \ \& \ A[p_i] \geq A[p_i - 1] \ \& \ A[p_i] > A[p_i + 1] \ , i = 1, 2, \cdots, M \tag{21}$$

where M is the number of peaks in the segment. For a segment size of 3 seconds, the corresponding number of beats ranges from 5 to 10 (the normal fetal heart beat is from 100 to 200 beat per minute). The resulting peak instants and the corresponding envelop values are then stored in set **P** and set **A** respectively

$$\mathrm{P} = \{p_1 \ , \ p_2 \ , \ \dots \ , \ p_M\}, \tag{22}$$

$$\mathrm{A} = \{A[p_1] \ , \ A[p_2] \ , \dots , A[p_M]\}, \tag{23}$$

2.4.3. S_1 Peak Selection

As we mentioned before, in many cases, S_1 and S_2 peaks are not easy to detect. On the contrary, in some low SNR signals, many fake peaks may present. For this reason, we propose to use some rules to select the potential S_1 peaks from **P** and **A**.

All the peaks are firstly reviewed in terms of their intervals. If there are some adjacent peaks which are less than 30 ms in between, as in [3], we merge them by using

$$p_{meg} = \frac{p_i A[p_i] + p_{i+1} A[p_{i+1}]}{A[p_i] + A[p_{i+1}]}, \tag{24}$$

$$A[p_{meg}] = \frac{A[p_i] + A[p_{i+1}]}{2}, \tag{25}$$

where p_i, p_{i+1}, $A[p_i]$ and $A[p_{i+1}]$ are the instants and the amplitudes of the two consecutive peaks to be merged. Subsequently, we remove p_i and p_{i+1} from **P** and $A[p_i]$ and $A[p_{i+1}]$ from **A** and replace them by p_{meg} and $A[p_{meg}]$, respectively.

Secondly, we select the most potential S_1 peaks based on their amplitude regularity. The instants satisfying the following condition are chosen as the next round candidates and saved in a new set **P'**.

$$\frac{A[p'_{i+1}]}{A[p'_i]} < \gamma \quad , \; i = 1,2,....,N-1 , \tag{26}$$

$$\mathbf{P}' = \{p'_1 \; , \; p'_2 \; , \dots , \; p'_N\} , \tag{27}$$

where γ is the ratio of two adjacent peaks in **P**' and is set to be $\gamma = 2$. N is the number of selected S_1 peaks.

2.4.4. Abnormal Interval Exclusion

The intervals between each two consecutive peaks in **P**' are denoted as

$$q_i = p'_{i+1} - p'_i \;\; , \;\; i = 1,2,....,N-1 \;\; , \tag{28}$$

and the interval set is denoted as **Q**

$$\mathbf{Q} = \{q_1 \; , \; q_2 \; , \dots , \; q_{N-1}\} , \tag{29}$$

We further remove those abnormal intervals from **Q** so that all the intervals used in the subsequent FHR calculation are within the predefined range. The final interval sets **Q'** with *K-1* elements are given by

$$\mathbf{Q}' = \{q'_1 \; , \; q'_2 \; , \dots , \; q'_{K-1}\} , \tag{30}$$

where K is the final S_1 peak number in the current segment, which may be equal or less than N, and

$$\frac{60F_S}{FHR_{\max}} < q'_i < \frac{60F_S}{FHR_{\min}} \quad , \; i = 1,2,...,K-1 , \tag{31}$$

where $FHR_{\min}$ = 100 BPM and $FHR_{\max}$ = 200 BPM.

After removing all the abnormal peaks and intervals, we resort **P**' and corresponding **A**'. The ultimate selected S_1 peak instants and envelop values are rewritten here as

$$\mathbf{P}' = \{p'_1 , \quad p'_2 , \quad \cdots , \quad p'_K\} , \tag{32}$$

$$\mathbf{A}' = \{A[p'_1] \; , \; A[p'_2] \; , \dots , \; A[p'_K]\} , \tag{33}$$

2.4.5. Fetal heart rate calculation

Regardless of occasional interference peaks, stronger peaks normally indicate more reliable measures. Therefore we highlight these cycles by weighting with their respective envelop amplitude $A[k]$. In the end the weighted fetal heart beat period T_w is obtained by

$$T_W[k] = \frac{\sum_{j=1}^{K-1} \left(A[p'_{j+1}] + A[p'_j] \right) q'_i}{\sum_{j=1}^{K-1} \left(A[p'_{j+1}] + A[p'_j] \right)} , \tag{34}$$

and the FHR is given by

$$FHR[k] = \frac{1}{T_w[k]}, \tag{35}$$

2.5. Confidence Factor

Due to the highly non-stationary characteristics of the fetal heart sound itself and the unforeseeable noise condition, the calculated FHR in some time may be more reliable than others. Through observing large amount of data captured in our clinical trial and their corresponding FHR results, we notice that the fetal heart sound needs to have a high SNR ratio with a series of *regular* and *distinct* peaks of $A[k]$ to guarantee a reliable FHR result.

So far little work has been done by which one can quantitatively evaluate the reliability of the resulted FHR during the real time monitoring. To start with, several parameters have been tested, such as the variance of $A[p_j]$, the variance of q_j and the consistency of the envelop peak shape. However, these indicators are not robust.

In the following we propose a spectrum distribution-based method to evaluate the regularity of the fetal heart sound. The method is mainly derived from the spectrum characteristics of the fetal heart signals with various levels of quality.

Let us first look at some examples as shown in Fig. 4. Here we list some fetal heart sound envelops and their normalized spectrum over 0 to 10 Hz. The normal fetal heart rate ranges from 1.67 Hz to 3.33 Hz, corresponding to 100 to 200 Beat-Per-Minute, as we highlighted in each figure. From Fig. 4, the following characteristics are observed:

(a) If the envelop is regular, there is usually a dominant and highest spectral peak within 1.67-3.33 Hz. The components below 1.67 Hz are relatively weaker. Some distinct and strong peaks at the FHR harmonic frequencies beyond 3.33 Hz may appear, like in Fig. 4(a)-(b).
(b) If the envelop is not regular, the peaks in 1.67-3.33 Hz may most likely become subordinate. There may be some other comparable peaks within and outside the 1.67-3.33 Hz, see Fig. 4(e)-(f).
(c) Sometimes the fetal heart sound is so weak that the maternal heart beat become the major component. In this case, there would be a strongest peak below 1.67 Hz, indicating the mother's heart rate (mother's heart rate in well condition is less than 120 BPM). The spectral peaks in the range 1.67-3.33 Hz are relatively lower and less distinct, see Fig. 4(g)-(h).

Although there may be some exceptional variations which are not strictly follow the rules as summarized above, they can be readily used to evaluate the signal quality. In the following, we will propose a spectrum distribution based scheme to quantify the above rules and provide a confidence factor ranging from 0 to 1 to evaluate the signal quality.

Fig. 5 shows a spectrum of the fetal heart sound envelop signal. To evaluate the distinctiveness of the dominant peak in 1.67-3.33 Hz, we propose an indicator using the area ratio (equivalent to power ratio) of the main lobe (the area within the dashed lines) to that of the bandwidth of interest 1.67-3.33 Hz marked as the shaded area. Please note that we use only the 1.67-3.33 Hz spectrum rather than the whole bandwidth as the benchmark. The reason lies in that there may be some strong harmonic peaks above 3.33 Hz, which does not necessarily indicate a poor signal, as mentioned earlier in the first characteristic.

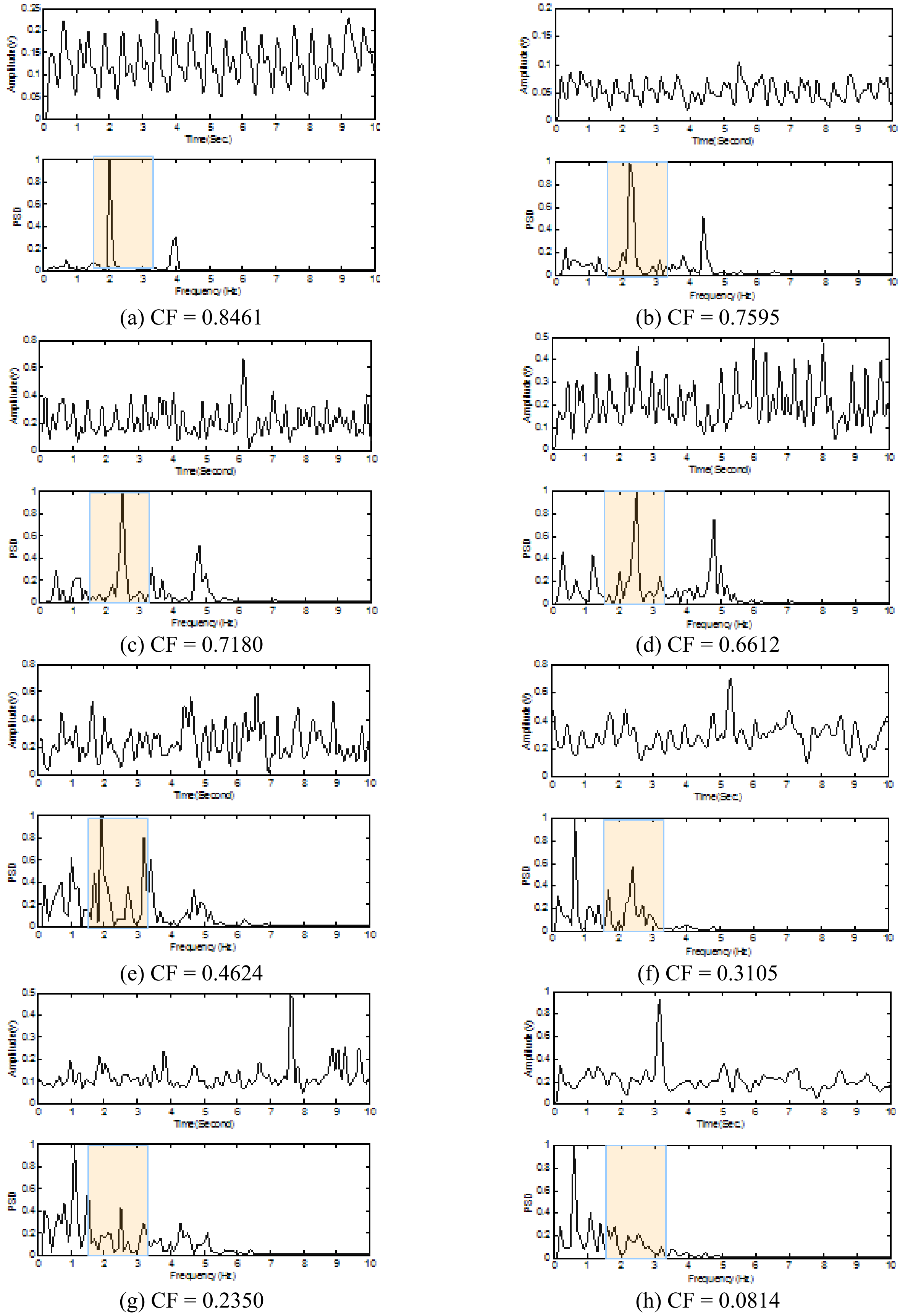

(a) CF = 0.8461

(b) CF = 0.7595

(c) CF = 0.7180

(d) CF = 0.6612

(e) CF = 0.4624

(f) CF = 0.3105

(g) CF = 0.2350

(h) CF = 0.0814

Fig. 4. Some examples of signal envelop and their corresponding spectrum at different quality levels. The upper one of each figure is the envelop signal of the fetal heart sound and the lower one is the spectrum over 0-10 Hz. Figure 4(a)-(h) are in decreasing order in terms of signal quality.

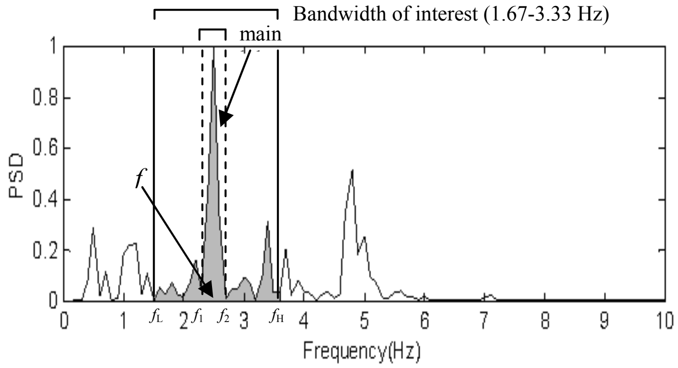

Fig. 5. Spectrum of a 10-second fetal heart sound envelop signal. The interested bandwidth is highlighted using shading colour and the main lobe is marked using two dashed lines.

Let us denote the Fast Fourier Transform of the fetal heart sound envelop $A[k]$ as $F_A(f)$

$$F_A(f) = FFT\{A[k]\}, \tag{36}$$

The power spectrum at each frequency is given by

$$P_A(f) = |F_A(f)|^2, \tag{37}$$

and the power of the envelop signal within f_L =1.67 Hz to f_H = 3.33 Hz is given by

$$E = \sum_{i=f_L}^{f_H} P_A(f_i). \tag{38}$$

Similarly, the power of the main lobe is

$$E_m = \sum_{i=f_1}^{f_2} P_A(f_i), \tag{39}$$

where f_1 and f_2 is the null frequencies beside the main lobe. If there is no null within this frequency range, we use $f_1 = f_L$ = 1.67 Hz and $f_2 = f_H$ = 3.33 Hz.

Subsequently, the distinctiveness factor of the peak within the 1.67-3.33 Hz can be defined as

$$\eta = \frac{E_m}{E}, \tag{40}$$

where η is a positive value ranging from 0 to 1. The higher the η, the more distinct the main lobe will be.

We will soon find that it is not sufficient by merely using η to evaluate the signal quality. In many cases, due to some strong spectral peaks below f_L, as the second characteristic mentioned above, high

η may not always indicate a good signal. Taking this into consideration, we adjust the confidence factor as

$$CF = \frac{E_m}{E} \cdot \frac{P_A(f_{m1})}{P_A(f_{m2})}, \tag{41}$$

where f_{m1} denotes the frequency corresponding to the maximum peak between f_L and f_H (see Fig. 5), f_{m2} denotes the frequency corresponding to the maximum peak between 0 and f_H. When the peak in f_L and f_H is the strongest one, the latter part in Eq. (40) reduces to 1, which means the additional term does not affect at all. On the other hand, when the peak below f_L is stronger, it normally indicates that the signal quality is not that good, see Fig. 4(h). In this case the second term is less than 1 and in turn reduces the value of CF proportionally.

The confidence factors of the signals shown in Fig. 4 have been calculated and given under the figures. It has been observed that the CF works reasonably well. For good quality signal, e.g., Fig. 4(a), the obtained CF is close to 1, while as the signal quality degrades, the corresponding CF decreases to almost 0.

3. Device Implementation and Clinical Trial

In this section, we give a brief description of our portable iPaq based fetal heart monitor, its main components and raised some practical issues in our development. Subsequently, the performance and the effect of those signal processing techniques introduced in Section 2 are further investigated by using the data collected from our clinical trials.

3.1. HP iPAQ hx4700 Portable Fetal Heart Monitor

Fig. 6 shows the design of our prototype using a HP iPaq hx4700. On the left of Fig. 6 is the Teflon-made inverse horn with a Panasonic omni-directional microphone embedded in its bottom. The preamplifier, two EL1CR2 3.0V batteries and the low pass filter circuit board are enclosed in the black box. The data acquisition unit, digital signal processing and display are performed on the iPaq. The HP iPaq hx4700 has an Intel XScale 624 MHz processor, 128MB Flash ROM, 64 MB SDRAM, 4" VGA color display and a 16 bit sound processor. The audio jack includes a microphone input and a stereo earphone so that we can capture the signal and play the processed signal in real-time.

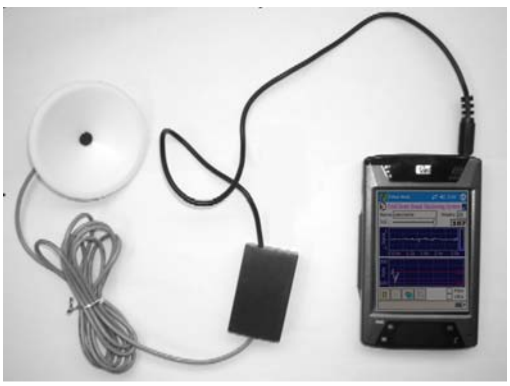

Fig. 6. A portable fetal heart monitor device using a HP iPaq hx4700, a white Teflon-made cone, a Panasonic omni-directional microphone, the preamplifier and filter analog circuit.

The user interface was developed using the Embedded VC++ 4.0 on the Pocket PC 2003 OS platform. The system can capture the signal from the sensors and display them on the LCD screen in real time. At the same time, all the signal processing modules are running behind the interface. The calculated FHR trace is shown below the signal waveform, as seen in Fig. 6. The user can hear the processed, clean fetal heart sound through an earphone (not shown in the figure). The confidence factor is displayed in different colors in the FHR trace, indicating the reliability of the current FHR result. The whole device is light, compact and easy to use.

3.2. Clinical Trial Results

Clinical experiments were carried out in a local hospital on 41 pregnant women who were about to give birth (37-38 weeks pregnant). Our sensor was placed just beside the CTG sensors and for each trial ten minutes data from both devices were recorded simultaneously for subsequent comparison. In the following we will investigate the performance of our device in terms of the clearness, the confidence factor and the FHR accuracy.

3.2.1. Clearness Issue

The clearness of the fetal heart sound is an important usability indicator for layman users. As introduced in Section 2, the clearness is improved by using the modified spectral subtraction followed by the AM/FM modulation. In the spectral subtraction method, the following parameters were adopted: $\alpha = 0.95$, $\beta = 0.7$. A comparison between the original waveform and the processed waveform is shown in Fig. 7. The processed signal shows much clear and distinct peaks and the AM modulation makes the sound much audible. According to the feedback from most of our users, these two measures improve the listening perceptual significantly.

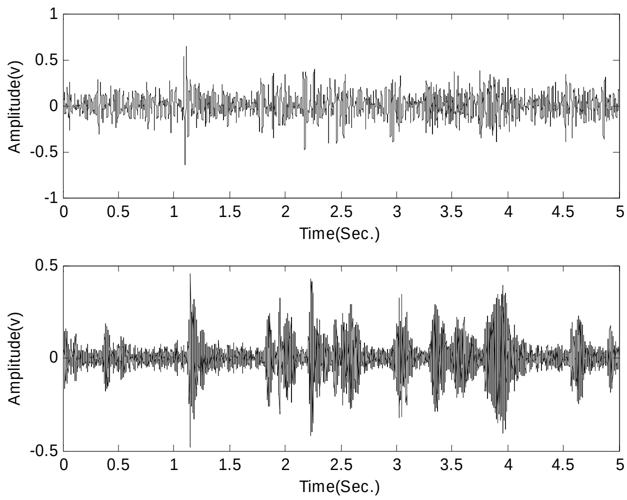

Fig. 7 Comparison between the original waveform (upper) and the processed waveform using the modified spectral subtraction and the AM modulation at 250 Hz carrier frequency (lower).

To quantitatively evaluate the performance of our device, the processed signals are subjectively classified into 5 grades with the Grade 1 being most unclear and the Grade 5 being the most distinct. A subjective listening testing was carried out by the pregnant women and our staff. The resulted clearness grade those 41 fetal heart sound signals is shown in Table 1.

Table 1. The result of clinical trial for the clearness investigation.

Grade	Number	Percentage
5: Very distinct & loud	17	41%
4: Distinct and loud	7	17%
3: Clear	7	17%
2: Need to listen attentively	6	15%
1: Cannot hear at all	4	10%
Total	41	100%

From Table 1 we observe that 75% of the fetal heart sound has a clearness level of 3 and above, indicating that most of these signals are clear and distinct. In contrast, it was shown that few pregnant women could identify their original fetal heart beat by listening to the *unprocessed* signals. In case when we could not hear the sound (Grade 1), we note that the pregnant mothers were very obese. This is not surprising as the CTG machine also experiences the same problem. Some other reasons may include the unfavourable or abnormal placenta position and the movement of the fetus, etc.

3.2.2. Confidence Factor (CF)

An experiment has been carried out to demonstrate the effectiveness of the confidence factor on a 150 second fetal heart sound signal. As can be seen in Fig. 8, the fetal heart sound varies greatly even during one minute. When some interference occurs, appearing as the sparkles in the signal envelop, the regularity of the signal degrades. In these cases, the CF value goes down immediately, indicating decreased signal quality and unreliable FHR calculation in that particular segment.

3.3. Fetal Heart Rate Accuracy Comparison

The experiments on synchronized comparison between *Sonicaid Fetal CTG* machine and our device have also been carried out. It is found that it would be less easy than CTG to get a long term stationary testing signal with distinct fetal heart beat, as the mother may move around, talk, or touch the device, which affects the continuity of our device. A typical result is shown in Fig. 9 to give a representation of how effective our system may work in normal conditions. It can be seen that aided with the confidence factor derived above, as highlighted in the figure using different colors, the users can perceive the reliability of the FHR results objectively. In most time, when the CF is high, our device functions well and provide results very close to the CTG records.

4. Conclusion

A portable fetal heart sound monitor has been developed on an HP iPaq hx4700. The processed fetal heart sound can be easily identified by layman users as well as gynecologists. Assisted with the confidence factor derived from the spectrum distribution, the reliability of the obtained FHR can be intuitively evaluated, by which the users can get their fetal heart rate reading more confidently and objectively. The confidence factor can in turn be used as an indicator to search the optimal fetal heart auscultation location.

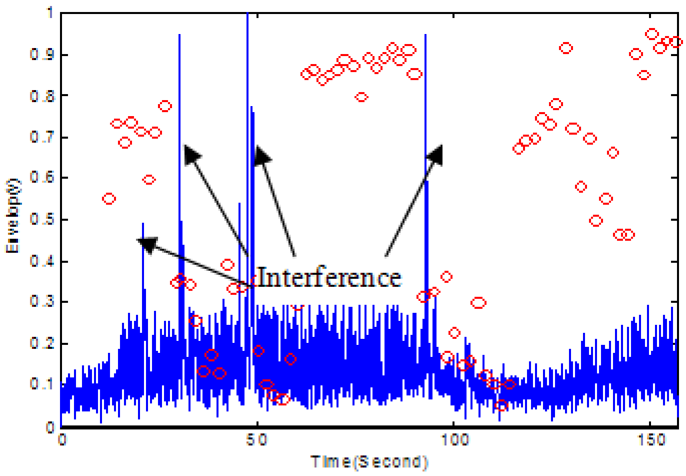

Fig. 8. 150-second normalized fetal heart sound envelop signal and the calculated confidence factor. (Note: the circles indicates the confidence factor value calculated using the previous 10 seconds data).

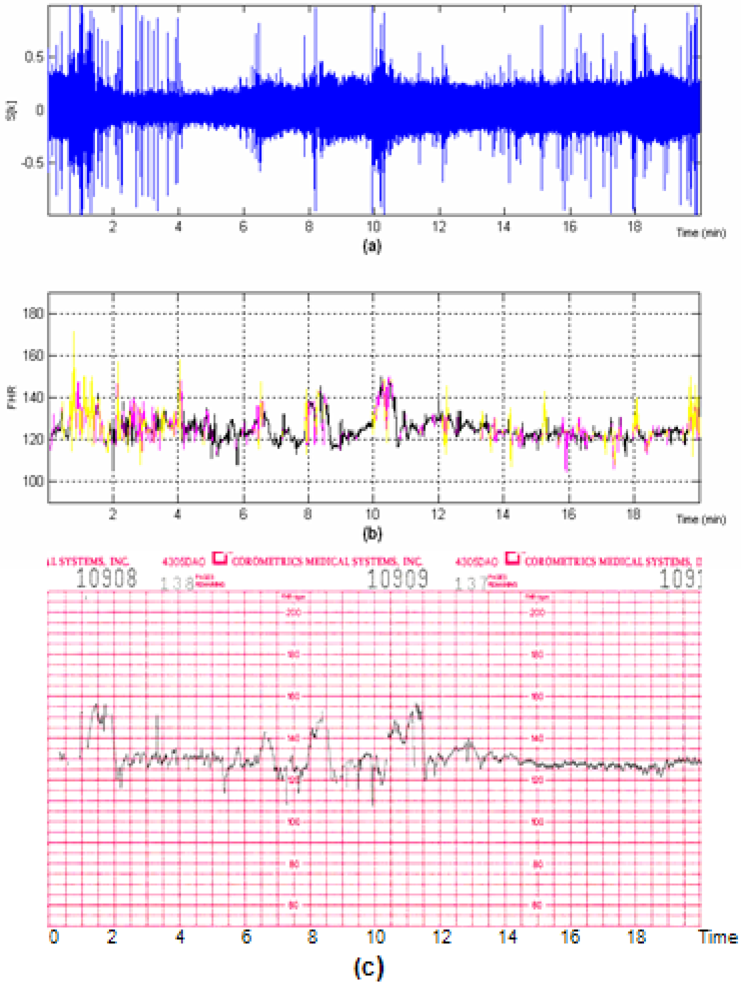

Fig. 9. Comparison of FHR traces obtained by our device and CTG machine. (a) 20 minutes original fetal heart sound data; (b) FHR trace obtained by our device; (c) FHR trace obtained by CTG machine. Note: the Confidence Factor is also demonstrated in (b) by different colours, Black: CF>0.7; Pink: 0.35<CF<0.7; Yellow: CF<0.35.

On the other hand, we realize that the performance of the fPCG is still not as good when compared to the fCTG, especially in high interference situations. Therefore we suggest using the device as a supplementary tool rather than a substitution for the ultrasound device. It can also be used as a prescription device at home or in office, especially during the last few weeks of pregnancy or for high risk pregnant women. Moreover, the device can also act as a preliminary data acquisition and processing device through which people can send the acquired fetal information to the doctor for advice and consultation via the state-of-the-art data communication technology. This telemedicine capability will play an even more important role in remote areas where obstetrics clinic may not be conveniently accessible. Ultimately, the proposed device will be a monitoring facility using telemedicine technique to transmit acquired fetal information for fetal status diagnostics.

References

[1]. R. K. Freeman, T. J. Garite, Fetal Heart Rate Monitoring, chapter The Physiologic Basis of Fetal Monitoring, *Williams and Wilkins*, Baltimore, Maryland, 1981, pp. 7-17.
[2]. D. M. Holburn, T. D. Rowsell, Real time analysis of fetal phonography signals using the TMS320, *IEEE Colloquium on Biomedical Applications of Digital Signal Processing*, 30 Nov 1989, pp. 7/1 –7/12.
[3]. P. Várady, L. Wildt, Z. Benyó, A. Hein, An advanced method in fetal phonocardiography, *Computer Methods and programs in Biomedicine*, 71, 2003, pp. 283-296.
[4]. F. Kovács, M. Török, I. Habermajer, A rule-based phonocardiographic method for long-term fetal heart rate monitoring, *IEEE Trans. Biomed. Eng*., 47, 2000, pp. 124-130.
[5]. D. G. Talbert, W. L. Davies, F. Johnson, N. Abraham, N. Colley, D. P. Southall, Wide bandwidth fetal phonography using a sensor matched to the compliance of the mother's abdominal wall, *IEEE Trans. Biomed. Eng*., Vol. 33, No. 2, 1986, pp. 175-181.
[6]. H. G. Goovaerts, H. P. van Geijn, O. Rompelman, An inductive sensor for recording of fetal movements and sounds, Proceedings of the *Annual International Conference of the IEEE Engineering in Medicine and Biology Society*, Vol. 13, No. 4, 1991, pp. 1622 –1623.
[7]. A. J. Zuckerwar, R. A. Pretlow, J. W. Stoughton, D. A. Baker, Development of a piezopolymer pressure sensor for a fetal heart rate monitor, *IEEE Trans. Biomed. Eng*., Vol. 40, No. 9, 1993, pp. 963-969.
[8]. N. Colley, D. G. Talbert, D. P. Southall, Biophysical profile in the fetus from a phonographic sensor, *European Journal of Obstetrics, Gynecology and Reproductive Biology*, Vol. 23, 1986, pp. 261-266.
[9]. J. Nagel, New diagnostic and technical aspects of fetal phonocardiography, *European Journal of Obstetrics, Gynecology and Reproductive Biology*, Vol. 23, 1986, pp. 295–303.
[10]. L. G. Durand, et al, Comparison of air and contact microphones for estimating the acoustic transmission of heart sounds in dogs, *Innov. Tech. Biol. Med*., Vol. 7, 1986, pp. 458-473.
[11]. H. G. Goovaerts, D. Cohen, J. H. Dripps, R. Mantel, P. Mooney, H. W. Jongsma, K. J. Dalton and H. P. van Geijn, A comparative clinical study of fetal phono- and movement-sensors from Amsterdam, Cambridge and Edinburgh, *Journal of Biomed. Eng*., Vol. 13, 1991, pp. 495-499.
[12]. M. Godinez, A. Jimenez, M. R. Ortiz, M. Peňa, On-line fetal heart rate monitor by phonocardiography, Proceedings of the *25th Annual International Conference of the IEEE Engineering in Medicine and Biology Society*, Vol. 4, 17-21 Sept. 2003, pp. 3141 - 3144
[13]. H. E. Bassil, J. H. Dripps, Real time processing and analysis of fetal phonocardiographic signals, *Clin. Phys. Physiol. Meas*., 10 (Suppl B), 1989, pp. 67-74.
[14]. A. Jiménez, M. R. Ortiz, M. A. Peňa, S. Charleston, R. González, A. T. Aljama, S. Carrasco, Performance of a method to generate fetal cardiotachograms using fetal phonocardiography, *Computers in Cardiology*, 28, 2001, pp. 453-456.
[15]. A. Jiménez, M. R. Ortiz, M. A. Peňa, S. Charleston, A. T. Aljama, R. González, Performance of two adaptive subband filtering schemes for processing fetal phonocardiograms: Influence of the wavelet and the level of decomposition, *Computers in Cardiology*, 27, 2000, pp. 427-430.
[16]. B. H. Tan, M. Moghavvemi, Real time analysis of fetal phonocardiography, Proc. *TENCON 2000*, Vol. 2, 2000, pp. 135 –140.
[17]. A. Jiménez, M. R. Ortiz, M. A. Peňa, S. Charleston, A. T. Aljama, R. González, The use of wavelet packets to improve the detection of cardiac sounds from the fetal phonocardiogram, *Computers in Cardiology*, 26, 1999, pp. 463-466.

[18]. A. Jiménez, S. Charleston, M. Peňa, A. T. Aljama, R. Ortiz, Performance of the Hilbert Transform in fetal phonocardiography for cardiotacogram generation, Proceedings of the *1st Joint BMES/EMBS Conference Serving Humanity, Advancing Technology*, Oct. 1999, Atlanta, GA, USA, p. 298.
[19]. F. Kovács, M. Török, An improved phonocardiographic method for fetal heart rate monitoring, Proceedings of the *20th Annual International Conference of the IEEE Engineering in Medicine and Biology Society*, Vol. 20, No. 4, 1998, pp. 1719-1722.
[20]. M. A. Peňa, R. Gonzalez, A. T. Aljama, S. Carrasco, R. Ortiz, C. G. Vargas, G. Valencia, Comparison of abdominal ECG and phonocardiography for instantaneous fetal heart rate detection, Proc. *IEEE-EMBC and CMBEC*, 1997, pp. 123-124.
[21]. F. Kovács, M. Török, An instrument using parallel filtering of acoustic signals to record fetal heart rate, *Biomedical Instr. And Techn*., Vol. 11, No. 3, 1995, pp. 213-219.
[22]. J. T. E. McDonnell, Knowledge-based interpretation of fetal phonocardiographic signals, *Inst. Elect. Eng Proc.*, pt. F, Vol. 137, No. 5, Oct. 1990, pp. 311–318.
[23]. K. L. Fernanndo, V. J. Mathews, M. W. Varner, E. B. Clark, Robust estimation of fetal heart rate variability using Doppler ultrasound, Proc. *ICASSP*, 2003, pp. II-257-260.
[24]. http://www.quantum-world.co.uk/information.
[25]. A. Baykal, Y. Z. Ider, H. Koymen, Use of signal averaging in analysis of the digital phonocardiograms, Proc. *Annual International Conference of the IEEE Engineering in Medicine and Biology Society*, Vol. 13, No. 5, 1991, pp. 2103-2104.
[26]. M. A. Tinati, A. Bouzerdoum, J. Mazumdar, Modified Adaptive Line Enhancement Filter and its Application to Heart Sound Noise Cancellation, Proc. on *International Symposium on Signal Processing and its Applications (ISSPA)*, Gold Coast, Australia, 25-30 August, 1996.
[27]. N. V. Thakor, Y. S. Zho, Application of adaptive filtering to EEG analysis: Noise cancellation & arrhythmia detection, *IEEE Trans. Biomedical Engineering*, Vol. 38, 1991, pp. 785-793.
[28]. Y. Lu, W. Liu, G. Qin, Removal of the heart sound noise from the breath sound, *IEEE Engineering in Medicine and Biology Society 10th Annual International Conference*, 1988, pp. 175-176.
[29]. Messer, S. R., Agzarian, J., Abbott, D, Optimal wavelet denoising for phonocardiograms, *Microelectronics Journal*, 32, 2001, pp. 931-941.
[30]. Varady, P., Wavelet-based adaptive denoising of phonocardiographic records, Proc. of the *23rd Annual International Conference of the IEEE Engineering in Medicine and Biology Society*, 2001, Vol. 2, 25-28 Oct. 2001, pp. 1846 –1849.
[31]. Rainer Martin, Noise power spectral density estimation based on optimal smoothing and minimum statistics, *IEEE Trans. On Speech and Audio Processing*, Vol. 9, No. 5, 2001, pp. 504-512.
[32]. Y. Ephram, D. Malah, Speech enhancement using a minimum mean-square error short time spectral amplitude estimator, *IEEE Trans. On acoustics, speech, and signal processing*, Vol. ASSP-32, No. 6, Dec. 1984, pp. 1109–1121.
[33]. Haghighi-Mood, A., Torry J. N., A sub-band energy tracking algorithm for heart sound segmentation, *Computers in Cardiology*, 10-13 Sept. 1995, pp. 501-504.
[34]. Davis, H., Silverman, S. R., Hearing and Deafness, *Holt, Rhinchart and Winston*, New York, 1978.
[35]. R. B. Northrop, Noninvasive instrumentation and measurement in medical diagnosis, Chapter 14, *CRC Press LLC*, 2002, p. 305.
[36]. B. P. Lathi, Modern Digital and Analog Communications Systems, 3rd Edition, *OUP*, 1998.

Guide for Contributors

Aims and Scope

Sensors & Transducers Journal (ISSN 1726-5479) provides an advanced forum for the science and technology of physical, chemical sensors and biosensors. It publishes state-of-the-art reviews, regular research and application specific papers, short notes, letters to Editor and sensors related books reviews as well as academic, practical and commercial information of interest to its readership. Because it is an open access, peer review international journal, papers rapidly published in *Sensors & Transducers Journal* will receive a very high publicity. The journal is published monthly as twelve issues per annual by International Frequency Association (IFSA). In additional, some special sponsored and conference issues published annually.

Topics Covered

Contributions are invited on all aspects of research, development and application of the science and technology of sensors, transducers and sensor instrumentations. Topics include, but are not restricted to:

- Physical, chemical and biosensors;
- Digital, frequency, period, duty-cycle, time interval, PWM, pulse number output sensors and transducers;
- Theory, principles, effects, design, standardization and modeling;
- Smart sensors and systems;
- Sensor instrumentation;
- Virtual instruments;
- Sensors interfaces, buses and networks;
- Signal processing;
- Frequency (period, duty-cycle)-to-digital converters, ADC;
- Technologies and materials;
- Nanosensors;
- Microsystems;
- Applications.

Submission of papers

Articles should be written in English. Authors are invited to submit by e-mail editor@sensorsportal.com 6-14 pages article (including abstract, illustrations (color or grayscale), photos and references) in both: MS Word (doc) and Acrobat (pdf) formats. Detailed preparation instructions, paper example and template of manuscript are available from the journal's webpage: http://www.sensorsportal.com/HTML/DIGEST/Submition.htm Authors must follow the instructions strictly when submitting their manuscripts.

Advertising Information

Advertising orders and enquires may be sent to sales@sensorsportal.com Please download also our media kit: http://www.sensorsportal.com/DOWNLOADS/Media_Kit_2008.pdf

Smart Sensors Systems Design

A five-day advanced engineering course

10-14 November 2008, Barcelona, Spain

SMARTSES

Marie Curie Chair (EXC) project

General Information

This course is suitable for engineers who design different digital and intelligent sensors, data acquisition, and measurement systems. It is also useful for researchers, graduate and post graduate students. Course will be taught in English.

Course Description

An advanced engineering course describes modern developments and trends in the field of smart sensor systems and digital sensors design.

After a general overview of data acquisition methods, modern smart, digital and quasi-digital sensors, smart systems details are discussed. A systematic approach towards the design of low-cost high-performance smart sensors systems with self-adaptation and self-identification possibilities is presented.

Contact Person

Susana Escriche
Fundació UPC. Edifici Vèrtex
Plaça Eusebi Güell, 6, 08034 Barcelona
Tel.: +34 93 401 08 94
E-mail: susana.escriche@fundacio.upc.edu

Course Instructor

Prof. Sergey Y. Yurish,
Centre de Disseny d'Equips Industrials (CDEI),
Universitat Politecnica de Catalunya (UPC-Barcelona)
Tel.: + 34 93 401 74 37, fax: + 34 93 401 19 89
E-mail: syurish@sensorsportal.com

Online Registration:
http://www.sensorsportal.com/HTML/SSSD_Course_2008.htm

Deadline for Registration:
31 October, 2008

Fundació UPC   MARIE CURIE ACTIONS   IFSA

www.sensorsportal.com